MOLECULAR AND CELLULAR BIOLOGY, Dec. 1982, p. 1501–1513
0270-7306/82/121501-13$02.00/0

Vol. 2, No. 12

Mutations at the *Saccharomyces cerevisiae SUP4* tRNA^{Tyr} Locus: Isolation, Genetic Fine-Structure Mapping, and Correlation with Physical Structure

JANET KURJAN† AND BENJAMIN D. HALL*
Department of Genetics, University of Washington, Seattle, Washington 98195

Received 12 March 1982/Accepted 17 September 1982

The *SUP4* tRNA^{Tyr} locus in Saccharomyces cerevisiae has been studied by the isolation and characterization of mutations at the *SUP4* gene which result in the loss of suppressor function. Most of the mutations act as single-site mutations, whereas about a third of the mutations are deletions of the entire gene. Two meiotic fine-structure maps of the gene were made. The first mapping technique placed 10 mutations plus the *sup4*$^+$ anticodon on a map by a measurement of levels of recombination between pairs of mutations. The second map utilized a more qualitative estimate of recombination frequency, allowing 69 mutations and the *sup4*$^+$ anticodon to be mapped. The maps were compared with the physical structure of the gene for the 34 mutations whose nucleotide alteration has been determined by DNA sequencing (Koski et al., Cell **22**:415–425, 1980; Kurjan et al., Cell **20**:701–709, 1980). Both maps show a good correlation with the physical structure of the gene, even though certain properties of genetic fine-structure maps, such as marker effects and "map expansion," were seen.

The use of genetic fine-structure mapping to order mutations within a gene has been based on the assumption that the recombination frequency between two mutations is proportional to the nucleotide distance between them. The first system in which this was actually tested was the tryptophan synthetase A gene in *Escherichia coli* (20). The results of that study indicated that the genetic fine-structure map was indeed colinear with the protein structure.

Since that time, it has become clear that fine-structure mapping in lower eucaryotic systems is subject to several features that put the accuracy of fine-structure maps into doubt. In yeasts, it has been found that both meiotic and mitotic X-ray fine-structure maps show "map expansion" (2, 3, 6, 9), a property initially defined by Holliday (7) in which, given a map order *abc*, the recombination frequency between *ac* is larger than that of the summed frequencies *ab* + *bc*. This property of map expansion indicates that the assumption that recombination frequency is proportional to DNA distance is not strictly true. Fine-structure mapping data also often show marker effects, in which a particular marker may give unusually high or low levels of recombination with other markers (3, 6). Such marker effects will also lead to inaccuracies in the fine-structure map.

† Present address: Department of Biological Sciences, Columbia University, New York, NY 10027.

Finally, an extensive study by Moore and Sherman (13, 14) indicated that the level of recombination per nucleotide could vary extensively between different pairs of mutations. These studies utilized a large number of mutations within the *Saccharomyces cerevisiae cyc1* gene for which the physical location of the mutations were known. Even two different mutations at the same site could give quite different levels of recombination with another mutation. This effect was significant enough to lead to improper ordering of mutations with respect to one another in some cases. Although this effect was shown to be significantly less extreme for meiotic recombination frequencies than for X-ray-induced mitotic recombination frequencies, enough variation was seen to cause difficulties in meiotic fine-structure mapping.

In this paper, we describe the isolation and characterization of second-site mutations at the *SUP* tRNA^{Tyr} locus in *S. cerevisiae*. We have made two meiotic fine-structure maps of these mutations. The first map, which includes 10 mutations and the *sup4*$^+$ anticodon, was made by the procedure of Rothstein (17, 18). For the second map, we made use of a qualitative plate assay for the determination of the relative frequencies of recombination between pairs of mutations, allowing the mapping of a large number of mutations. Elsewhere, we have reported the nucleotide alterations for a number of these

mutations (10, 11). We present here the comparison between the two genetic maps and the physical structure of the gene.

MATERIALS AND METHODS

Strains. The *S. cerevisiae* strains used in this analysis were J12-9A (*MATα ade2-1 lys2-1 trp5-2 leu1-12 can1-100 met4-1 ura1-1*), J15-8D (*MATα SUP4-0 ade2-1 lys2-1 trp5-2 leu1-12 can1-100 met4-1 ura1-1*), and J15-13C (*MATα SUP4-0 ade2-1 lys2-1 trp5-2 leu1-12 can1-100 met4-1 ura3-1*). These strains are haploid segregants from strains W87 and 164RW87 (19), which were provided by R. Rothstein.

Media. The media used were as follows, with addition of 1.5% agar (Difco) to prepare solid media.

(i) Complex media. YEP contained 1% yeast extract (Difco), 2% peptone (Difco), 2% glucose, 10 μg of adenine per ml, and 40 μg of uracil per ml. YPA medium contained 1% yeast extract, 2% peptone, and 2% potassium acetate, supplemented with 80 μg each of adenine, uracil, leucine, lysine, methionine, and tryptophan per ml.

(ii) Synthetic media. Minimal medium contained 0.17% yeast nitrogen base without amino acids (Difco) and 2% glucose. For complete medium the following supplements were added: adenine sulfate (10 μg/ml), leucine (100 μg/ml), methionine (20 μg/ml), lysine (50 μg/ml), tryptophan (50 μg/ml), and uracil (20 μg/ml), adjusted to pH 7. Dropout media were identical to the complete medium with the omission of one or two of the supplements. Canavanine medium was complete medium plus 80 μg of canavanine sulfate per ml, except where specified otherwise.

(iii) Sporulation medium. Sporulation medium contained 2% potassium acetate, 0.25% yeast extract, and 0.1% glucose and was supplemented with 75 μg each of adenine sulfate, leucine, lysine, methionine, tryptophan, and uracil per ml and adjusted to pH 7 with acetic acid.

Genetic techniques. Growth, replica plating, mating, dissection of asci, and scoring of genetic traits were performed as described by Mortimer and Hawthorne (15). Sporulation was done as described by Rothstein (17).

Mutant isolation. In the first mutant hunt, mutants were isolated by spreading 10^6 cells of J15-8D on plates containing 30, 50, 70, or 90 μg of canavanine per ml. In the second mutant hunt, independent clones of J15-8D and J15-13C were picked onto masters and then replica plated to several canavanine plates. A single pink or red canavanine-resistant colony was picked from each clone.

Determination of relative recombination frequencies. Fifty mutants isolated in J15-8D were crossed to 48 mutants isolated in J15-13C. The diploids were replica plated to sporulation medium and after 3 days at 30°C were replicated to medium lacking lysine and methionine or, in some cases, to medium lacking adenine and lysine. After 3 days on plates lacking lysine and methionine, or 5 days on plates lacking adenine and lysine, the frequency of papillations was scored.

Meiotic fine-structure mapping. Mutants to be mapped were first obtained in the opposite mating type by dissection of crosses to the parent of the opposite mating type.

(i) Fine-structure map 1. The procedure of Rothstein (17) was followed for the first fine-structure map. All possible intercrosses were made between 10 mutant strains and a *sup4*$^+$ strain. Each diploid was inoculated into 2 ml of YPA medium (which allows cells to grow to stationary phase and then sporulate) at 5×10^4 cells per ml. The culture was shaken at 30°C in a New Brunswick air shaker. After 2 days, before any asci had formed, appropriate dilutions were plated on complete medium and medium lacking lysine and methionine to determine the background frequency of mitotic recombination. After 6 days, when sporulation was complete, dilutions were plated to determine the frequency of mitotic recombination plus meiotic recombination. The mitotic recombination frequency was then subtracted to give the meiotic recombination frequency between the two mutations.

(ii) Fine-structure map 2. For the second fine-structure map, all possible intercrosses were made between 69 mutant strains and a *sup4*$^+$ strain, and the frequency of meiotic recombination was determined by spot tests as described above.

RESULTS

Mutant isolation. The mutant isolation scheme utilized two of the ochre-suppressible markers in strains J15-8D and J15-13C (*can1-100* and *ade2-1*), as described by Rothstein (17). Canavanine is a toxic arginine analog, preventing growth of cells on canavanine medium. The *can1-100* mutation is an ochre-suppressible mutation in the arginine permease which renders cells resistant to canavanine (5). The ochre suppressor *SUP4* in combination with the *can1-100* mutations results in a canavanine-sensitive phenotype. Second-site mutations within the *SUP4* tRNA which abolish tRNA function lead to loss of suppression and can therefore be obtained by selection for canavanine resistance (2a, 12, 17). The *ade2-1* mutation provides a means of distinguishing loss-of-suppression mutations from new canavanine resistance mutations. The *ade2-1* mutation leads to the build-up of a red pigment, and suppression of the mutation results in a white phenotype. Loss-of-suppression mutants thus exhibit a red or pink phenotype. In this study, red and pink canavanine-resistant colonies were chosen for further analysis.

To distinguish mutations at the *SUP4* locus from unlinked antisuppressors, the mutants were crossed to a *sup4*$^+$ strain and the diploids were tested for the ability to segregate *SUP4* recombinants after sporulation. Mutations unlinked to *SUP4* segregate *SUP4* at a high frequency, whereas second-site mutations at *SUP4* only segregate a very low frequency of *SUP4* recombinants.

Mutant phenotypes. Various levels of residual suppression in the mutants are indicated by color phenotypes which range from light pink (high residual suppression) to red (no residual

TABLE 1. Mutants used in fine-structure mapping and deletion analysis

Mutant[a]	Residual suppression[b]	Mapping results[c]	Mutant[a]	Residual suppression[b]	Mapping results[c]
M16	+	II	M97	−	Deletion
M49	−	VIII	M98	−	IV
M50	+/−	IV	M99	−	VI
M51	+/−/−	VI	M100	+/−	V
M52	+/−	I	M101	+/−/−	II
M53	−	Deletion[d]	M102	+/−/−	X
M54	+/−	V	M104	+/−/−	VI, VII
M55	+/−	V	M105	+/−	III
M56	+/−/−	IX	M106	+/−	IV
M57	+/−	V	M107	+/−	I
M59	−	IX, X	M108	+/−	VII
M60	−	(I), II, (III)	M109	+/−	V
M61	−	II	M110	+	VI
M62	−	Deletion	M112	−	(II), III
M63	−	II	M113	−	VI
M64	−	IX, X	M116	−	Deletion
M65	−	Deletion	M117	−	Deletion
M66	−	IX	M118	−	(II), III
M67	−	Deletion	M119	−	IV
M68	−	II	M120	−	II
M69	−	I	M121	−	III
M70	−	VIII	M122	−	Deletion[d]
M71	−	Deletion[d]	M123	−	I
M72	−	Deletion	M124	−	II
M73	−	Deletion	M125	−	IV
M74	−	Deletion	M126	−	VII
M75	−	Deletion	M127	−	(IX), X
M76	−	Deletion	M128	−	IV
M77	−	IX	M129	+/−/−	IX
M78	−	Deletion[d]	M130	−	(IX), X
M79	−	IX	M131	−	IX, X
M80	−	Deletion	M132	−	Deletion
M81	−	Deletion	M133	−	IX
M82	−	III	M134	−	II, (III)
M83	−	II	M135	−	(VI), VII
M84	+/−/−	II	M136	−	(II), III
M85	−	Deletion	M137	−	VIII
M86	−	II	M138	−	II
M88	−	VII	M139	−	III
M89	−	Deletion[d]	M140	−	Deletion
M90	+/−/−	IV	M141	−	Deletion[d]
M91	−	I, II	M142	−	IX, X
M92	−	Deletion	M143	−	VIII
M93	−	Deletion	M144	−	III
M94	−	III	M145	−	I
M95	−	VII	M146	−	X
M96	−	VII			

[a] Mutants 16 and 49 to 98 were isolated in J15-8D; mutants 99 to 148 were isolated in J15-13C.

[b] Symbols: +, growth on medium lacking methionine in 1 day, growth lacking lysine in 3 to 5 days; +/−, growth without methionine in 2 to 3 days; +/−/−, growth without methionine in 4 to 5 days; −, no residual suppression.

[c] Roman numerals refer to clusters as shown in Fig. 6. Deletions were determined by genetic analysis.

[d] Also shown to be deletions by molecular analysis (16).

suppression) and by varying levels of growth on dropout media testing for the suppressible nutritional markers. The majority of the unlinked antisuppressors are very leaky, resulting in a high level of residual suppression, whereas the mutations at *SUP4* result in a much lower level of residual suppression, indicating that the mutations at the $tRNA^{Tyr}$ gene severely affect tRNA

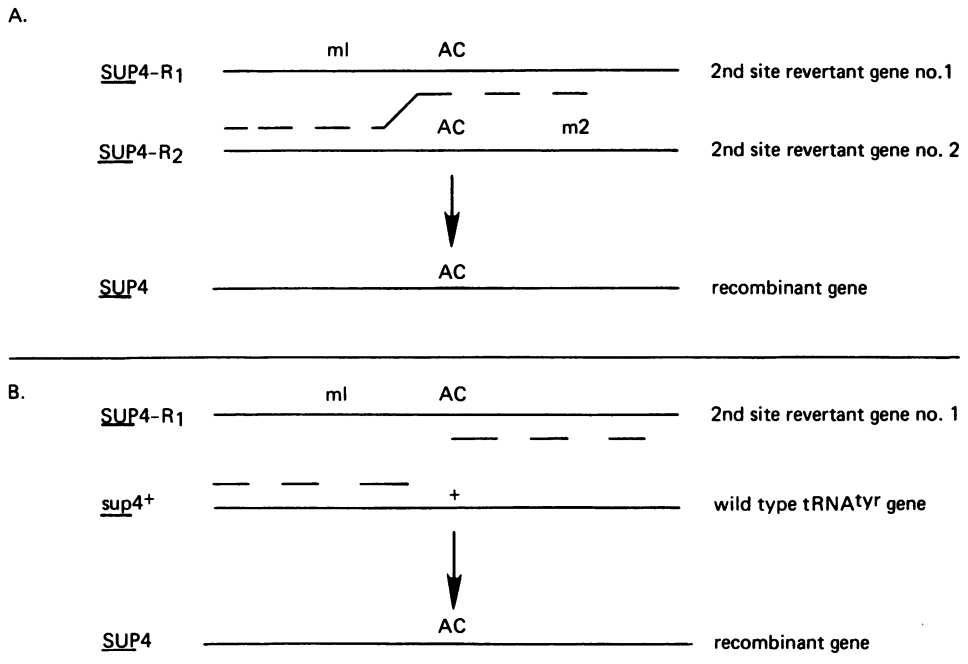

FIG. 1. Illustration of the formation of *SUP4* recombinants in a diploid heteroallelic for two second-site revertants (A) or heteroallelic for a second-site revertant and *sup4*$^+$ (B). AC, *SUP4* ochre anticodon; +, *sup4*$^+$ anticodon; *m1* and *m2*, second-site mutations. Dashes indicate recombination event.

function. Of the mutations which are allelic to *SUP4*, about 5% show slight suppression of the *met4-1* allele, and less than 1% also show slight suppression of the *lys2-1* allele. Those mutants which were analyzed further are listed in Table 1.

Deletion analysis. In a study of second-site revertants at the *SUP4* locus, Rothstein (18) found that a significant proportion of the revertants were deletions of the entire gene, whereas no deletions were found among *SUP3* second-site revertants (17). An analysis was undertaken to determine whether or not the *SUP4* revertants isolated in this study demonstrate this property. A mutation within the suppressor gene is able to recombine meiotically with a second mutation or with *sup4*$^+$ to give a *SUP4* recombinant, as described by Rothstein (17, 18) and illustrated in Fig. 1. Deletions of the entire gene result in a total lack of *SUP4* recombinants in a diploid heteroallelic for a deletion and any of the mutations at *SUP4*.

The mutants were tested for the ability to recombine with other *SUP4* second-site mutations by making crosses between 50 mutants isolated in J15-8D and 48 mutants isolated in J15-13C and testing by plate assays for the ability to form *SUP4* recombinants (data not shown). All 98 mutants were also crosses to *sup4*$^+$. Eighteen of the 98 mutants were unable to recombine with any of the mutants of the opposite mating type, indicating that they are deletions of the entire gene. A molecular analysis has confirmed that 6 of the 18 putative deletion strains actually have lost the entire $tRNA^{Tyr}$ gene plus a significant amount of flanking DNA (16) in a manner similar to that seen by Rothstein (18).

Meiotic fine-structure mapping. The meiotic fine-structure mapping procedures are based on the expectation that *SUP4* recombinants should be recovered at a frequency proportional to the nucleotide distance between the two second-site mutations (in a *SUP4-m1/SUP4-m2* diploid) or between a second-site mutation and the anticodon (in a *sup4*$^+$*/SUP4-m* diploid) as illustrated in Fig. 1. By comparing the frequencies of *SUP4* recombinants formed in all pairwise crosses between a set of mutants, two meiotic fine-structure maps were constructed. We have included *sup4*$^+$ in both maps to map our second-site mutations with respect to the anticodon.

Meiotic fine-structure map 1. Meiotic recombination frequencies between mutations were determined by the procedure of Rothstein (17, 18). The frequencies of *SUP4* meiotic recombinants for intercrosses between 11 *SUP4* alleles lacking

TABLE 2. Meiotic recombination frequencies[a]

Mutant	No. of recombinants per 10^5 asci										
	M52	M91	M84	M83	(M50	*sup4*$^+$)	M54	M55	(M59	M77	M79)
M52	0.6	2.2	3.6	6.7	17.8	7.0	9.3	26.5	32.7	33.4	49.7
M91	2.2	0.1	0	1.1	11.2	3.6	3.9	9.9	20.2	21.0	48.3
M84	3.6	0	0	0.7	8.3	4.1	2.1	8.4	40.9	20.4	31.2
M83	6.7	1.1	0.7	0.1	6.1	4.1	3.4	10.1	31.0	9.8	28.6
M50	17.8	11.2	8.3	6.1	0	0.3	1.8	10.1	30.8	72.1	47.4
sup4$^+$	7.0	3.6	4.1	4.1	0.3	—	0.3	2.1	11.6	6.0	21.8
M54	9.3	3.9	2.1	3.4	1.6	0.3	0	0	11.1	7.9	7.8
M55	26.5	9.9	8.4	10.1	10.1	2.1	0	0	3.9	6.5	11.6
M59	32.7	20.2	40.9	31.0	30.8	11.9	11.1	3.9	0.1	0	0.1
M77	33.4	21.0	20.4	9.8	72.1	6.0	7.9	6.5	0	0.6	0
M79	49.7	48.3	31.2	28.6	47.4	21.8	7.8	11.6	0.4	0.1	0.4

[a] Frequencies of meiotic recombinants on medium lacking lysine and methionine minus the mitotic background frequency. The data have been arranged such that the order of the mutations from left to right and from top to bottom is that of the final map as described in the text. Parentheses in column heads indicate that ordering of those mutations was not possible.

suppression (including *sup4*$^+$) are shown in Table 2.

The meiotic map order was derived by the method described by Rothstein (17). First, the recombination frequencies were examined for all triplets of mutants, *a*, *b*, and *c*, where one of the three strains was *sup4*$^+$. A map order *abc* was determined, such that *ac* showed a larger recombination frequency than *ab* or *bc*. In this way, the two mutants were placed either on the same side or opposite sides of the anticodon. By a comparison of these results for all triplets including the anticodon, the mutants were divided into groups on opposite sides of the anticodon. Mutants M52, M83, M84, and M91 map to one side, chosen arbitrarily to be the left side of the anticodon. Mutants M54, M55, M59, M77, and M79 map to the right side. Mutant M50 mapped so closely to the anticodon that it was impossible to place it on one side or the other. Of the 36 arrangements determined for triplets including *sup4*$^+$ and pairs of mutants (excluding triplets containing mutant M50), 31 are in good agreement with the final arrangement, 2 are ambiguous, and 3 are in disagreement with this arrangement.

The next step was to make maps of each half of the gene. Mutant M50 and *sup4*$^+$, which map very close to one another, were considered to be the middle of the gene and were included in both halves. In this case, all possible triplets were compared, excluding those triplets containing both M50 and the anticodon, and a map order was determined that agreed with the majority of the triplet combinations. The two halves of the map were then combined. Finally, the recombination frequency data were rearranged such that the mutants are in the order determined by the mapping results, in a manner similar to that used by Jones (9) and Cooper et al. (2). The data in Table 2 are shown in this rearranged order. For any given mutation, the lowest recombination frequency should be seen in combination with itself, and the recombination frequencies should increase towards both ends of the map. Although discrepancies are seen, this arrangement of the data aided in the placement of some closely linked markers. In some cases in which ordering of closely linked markers was difficult, comparison of recombination frequencies with flanking markers made ordering possible. It was not possible to order mutant M50 with respect to the anticodon mutation or mutants M59, M77, and M79 with respect to one another. Two marker effects can be seen in these data. Mutant M77 showed a somewhat higher level of production of recombinants in the cross to itself than it did in the crosses to the nearby markers, M59 and M79. DNA sequencing results (11) showed that mutation M77 is a deletion of a single cytosine residue from a tract of five cytosines near the 3′ end of the gene. Such a mutation should be able to give rise to *SUP4* recombinants at a low frequency by mismatch pairing within the tract of four guanine-cytosine base pairs remaining, thus explaining the high level of recombinants seen in the M77 self-cross. Also, as described below, the M77 deletion seems to inhibit recombination with nearby mutations, resulting in low levels of recombination with mutations M59 and M79. Mutant M50 gives a high level of recombinants with most of the other mutants, making its placement difficult. It was placed near to the anticodon based on its very low level of recombination with *sup4*$^+$. Although the recombination frequencies are high, they are in agreement with this placement, since they increase steadily towards both ends

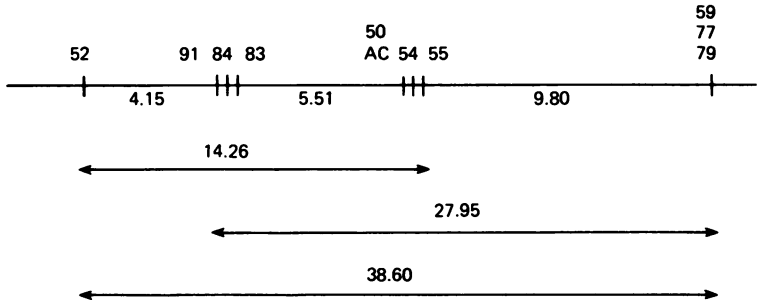

FIG. 2. Meiotic fine-structure map of *SUP4* based on the recombination frequencies shown in Table 2. Distances shown are the average distance between all members of the two clusters indicated (excluding mutant M50) and are given in recombinants per 10^5 asci. AC, Anticodon.

of the map as can be seen in Table 2. The final map is shown in Fig. 2. This map order shows good agreement with the data, as indicated by comparison of the orders determined by all possible triplets with the final map order. Of 131 triplets, 97 agree with this order, 10 are ambiguous, and 24 disagree. However, 8 of the ambiguities and 11 of the disagreements involve mutant M50 and thus are due to the marker effect shown by this mutation. Similar marker effects were seen in the fine-structure mapping of second-site tRNA mutations in *Schizosaccharomyces pombe* (6).

Our final map does exhibit map expansion (Fig. 2). The degree of map expansion can be visualized by plotting, for all triplets with map order *abc*, the observed recombination frequency for *ac* versus the expected frequency *ab* + *bc* (3), as has been done in Fig. 3. The line on the graph is that upon which the points would fall if

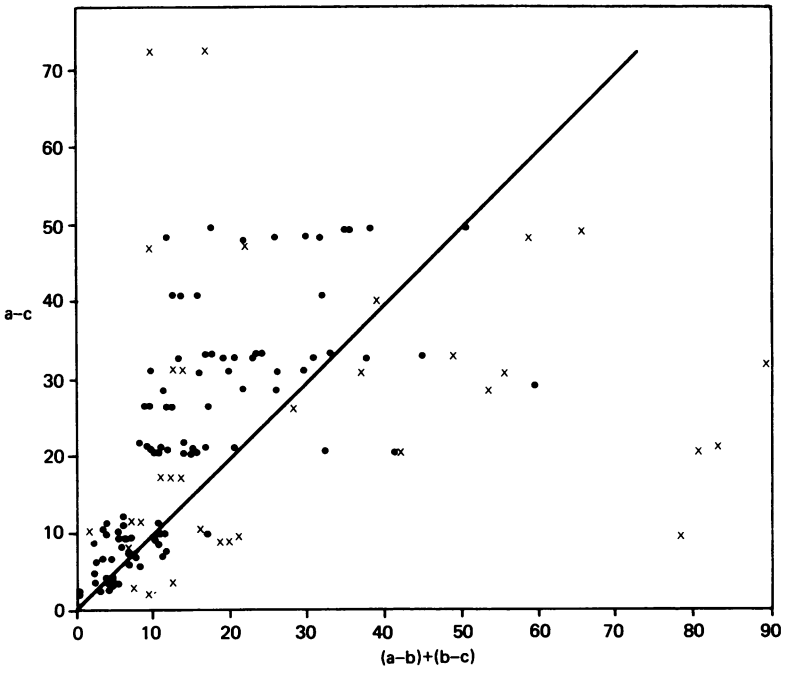

FIG. 3. Degree of map expansion, examined by plotting the observed frequency of recombination *ac* between the outer two members of a triplet with map order *abc* versus the expected frequency, *ab* + *bc*, for all possible triplets. Cases in which mutant M50 is included in a triplet are indicated by ×. The line represents that expected if the observed frequencies equaled the expected frequencies.

TABLE 3. Mutants with known nucleotide alteration

Mutant[a]	Original name	Suppression phenotype[b]	Map position	Distance from 5' end of gene (nucleotides)	Nucleotide change[c]
A1	M145	−	I	1	C → A
U3	M52, M107	+/−	I	3	C → U
G3	M123	−	I	3	C → G
U6	M69	−	I	6	G → U
G9	M105	−	III	9	A → G
U10	M91	−	I, II	10	G → U
G14	M60	−	(I), II, (III)	14	A → G
U15	M83	−	II	15	G → U
U21	M112	−	(II), III	23	A → U
G27	M94	−	III	29	C → G
U29	M106	+/−	IV	31	A → U
U30	M98	−	IV	32	G → U
G32	M50	+/−	IV	34	C → G
A32	M90	+/−/−	IV	34	C → A
U32	M125	−	IV	34	C → U
SUP4	Anticodon mutation		IV	36	U → G
C35	M128	−	IV	37	U → C
–A36, A37	M119[d]	−	IV	38–39	ΔAA
G37	M54, M109	+/−	V	39	A → G
U (IV)	M55, M57, M100	+/−	V	43	A → U
A40	M99, M113	−	VI	56	C → A
A45	M110	+	VI	61	G → A
G46	M51	+/−/−	VI	62	A → G
U51	M95	−	VII	67	G → U
A51	M108	+/−	VII	67	G → A
A52	M88	−	VII	68	C → A
G56	M70	−	VIII	72	C → G
U56	M137	−	VIII	72	C → U
G60	M49	−	VIII	76	U → G
C62	M79, M129	+/−/−	IX	78	G → C
–C(63–67)	M77[d]	−	IX	79–83	ΔC
U67	M56	+/−/−	IX	83	C → U
C68	M59	−	IX, X	84	G → C
A72	M127	−	(IX), X	88	G → A
U73	M102	+/−/−	X	89	A → U

[a] Mutants are named according to their position in the tRNA and their nucleotide alteration, as described by Celis (1). The tRNA numbering system of Sprinzl et al. (19a) is used. This system only assigns an integral number to those nucleotides of the D loop which correspond to nucleotides always present in the D loop, which differs in size among various tRNAs. The intervening sequence is not included. The intervening sequence mutation is numbered in roman numerals according to its position in the intervening sequence.

[b] Suppression phenotype as described in Fig. 1.

[c] Nucleotide changes are shown as they differ from the *SUP4* suppressor $tRNA^{Tyr}$ sequence.

[d] Mutation M119 is a deletion of two base pairs. Mutation M77 is a deletion of one guanine-cytosine base pair from a tract of five guanine-cytosine base pairs.

the observed values were equal to the expected values. The majority of the points fall above the line, indicating that this map has a tendency towards map expansion, as has been found for other meiotic fine-structure maps in yeasts (3, 6, 9).

Genetic map versus physical structure. To facilitate further study of these mutants with regard to their molecular defect, it is useful to know the approximate position of each mutation within the gene coding for the *SUP4* $tRNA^{Tyr}$ molecule. The fine-structure maps can provide this information, once the positions of several of the mutations on the map have been determined. We have determined the degree of correspondence by comparing fine-structure map 1 with the nucleotide position of those mutations whose mutational alteration has been determined by DNA sequencing (10, 11; R. Koski, S. Goh, and M. Smith, personal communication). Those mutants for which the nucleotide alteration is known are shown in Table 3. Figure 4 shows the correlation between nucleotide position and genetic map position for 10 of 11 of the mutations on map 1. Although the points do not fall directly on a line, it is clear that the map

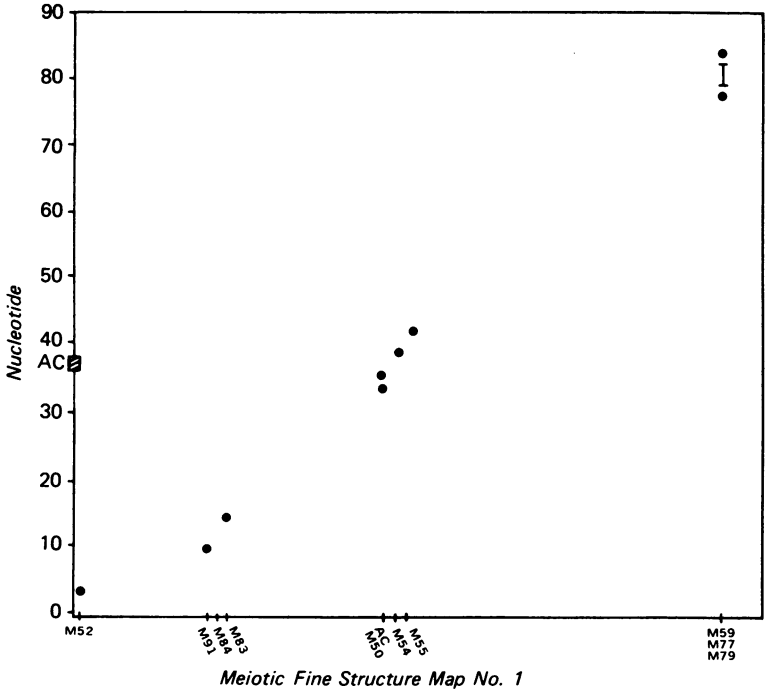

FIG. 4. Nucleotide position of the mutational changes versus fine-structure map 1, shown for the 9 of 10 second-site mutations whose nucleotide alteration has been determined (10, 11). The position of the *SUP4* anticodon mutation (AC) is also indicated. The vertical bar represents mutation M77, which is a deletion of a single cytosine from a tract of five cytosines extending from nucleotide 79 to nucleotide 83.

shows colinearity with the position of the mutations within the gene.

Recombination frequency per nucleotide. The recombinant frequencies per nucleotide for those mutants mapped by the first technique are shown in Table 4. Because mutant M77 is a deletion of a single cytosine residue from a tract of five cytosines within the $tRNA^{Tyr}$, the distance of the mutation from the other mutations is somewhat ambiguous. The frequencies for the single base substitution mutations are also shown in Table 4. The recombination frequencies have a mean and standard deviation of 0.371 ± 0.256 recombinant per 10^5 asci per nucleotide. Those diploids showing a recombination frequency outside the standard deviation are indi-

TABLE 4. Recombination frequency per nucleotide[a]

Mutant	Recombinants per 10^5 asci								
	M91	M83	M50	AC	M54	M55	M79	M59	M77
M52	0.310	0.497	0.574	0.211	0.259	0.662*	0.663*	0.404	0.417 –0.439
M91		0.133	0.465	0.138	0.136	0.299	0.710*	0.273	0.288 –0.305
M83			0.380	0.225	0.162	0.404	0.477	0.469	0.151 –0.161
M50				0.160	0.316	1.123*	1.077*	0.615	1.472*–1.603
AC					0.108*	0.294	0.570	0.241	0.127 –0.138
M54						0*	0.284	0.247	0.180 –0.198
M55							0.330	0.095*	0.163 –0.181
M79								0.059*	0.013*–0.065
M59									0.004*–0.018

[a] The recombination frequencies in recombinants per 10^5 asci per nucleotide for those mutants from the first meiotic map which have been sequenced (Table 3) are shown. The frequencies for the single-base substitution mutants are given, with the mutants listed in the order of the position of their alteration within the gene. Also given are the frequencies for mutant M77, a deletion of a single cytosine residue from a tract of five cytosines with the frequency determined from the first and last member of the tract of five. Frequencies outside the standard deviation are indicated by an asterisk.

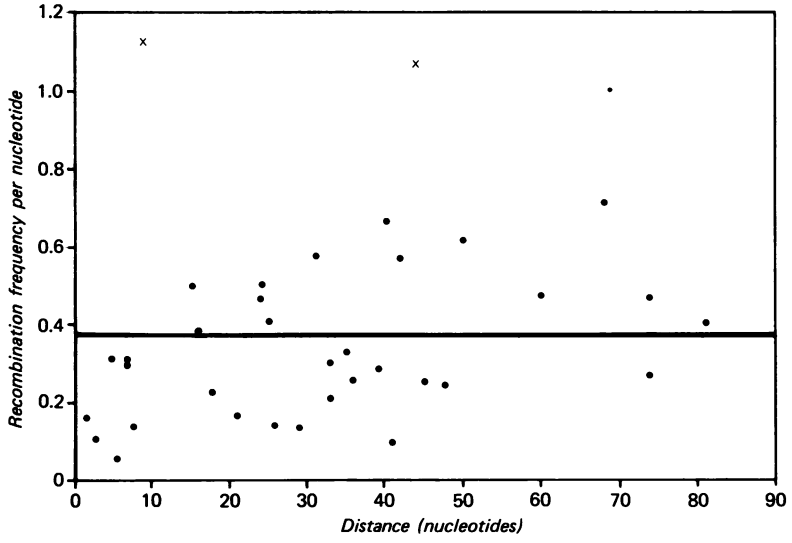

FIG. 5. Recombination frequencies per nucleotide from Table 4, plotted as a function of the nucleotide distance between the two mutations. The line represents the average frequency of 0.371 recombinant per 10^5 asci per nucleotide.

cated with an asterisk. Several marker effects are apparent. Two mutations near the left-hand end of the map, M52 and M91, show slightly high recombination frequencies with two mutations in the right half of the map, M55 and M79. Two mutations, M54 and M59, show unusually low levels of recombination with their immediate neighbors, resulting in difficulties in the ordering of mutations in this region. The most extreme marker effect is shown by mutation M50, consistent with the marker effect seen directly in the mapping data. This mutation gives very high frequencies with mutations to its right in the map, beginning with mutation M55, continuing through mutations M79 and M77, and dropping off to within the standard deviation with mutation M59. The deletion mutation M77 shows very low levels of recombination with its flanking markers, M59 and M79, suggesting that the deletion inhibits recombination within its vicinity.

Since fine-structure mapping is based on the assumption that the recombination frequency is proportional to the distance between two mutants, it is important to examine the validity of this assumption. Figure 5 shows the recombination frequencies per nucleotide plotted versus the distance between mutations. If this assumption is correct, the points should fall along the line representing the average frequency of recombination per nucleotide. Figure 5 indicates that there is a great deal of scatter in the recombination frequencies per nucleotide. There is a slight tendency for the recombination frequencies per nucleotide to increase somewhat as the distance between the two mutations increases (i.e., most of the points on the left-hand side of the graph fall below the mean frequency, whereas most of the points to the right fall above this frequency). This result is consistent with the notion that fine-structure maps show map expansion.

Meiotic fine-structure map 2. To facilitate mapping of a large number of mutations, a more qualitative form of meiotic fine-structure mapping was used. All possible intercrosses were made between 70 mutants (including a *sup4*$^+$ strain). Determination of the frequency of recombination between any two sites was done by replicating the diploids to sporulation medium and then replicating the sporulated material to double dropout medium selecting for *SUP4* recombinants. The diploids were assigned a recombination value from 0 to 5 based on the frequency of papillation on the double dropout medium, as follows: (0) 0 papillations, (1) 1 to 5 papillations, (2) 6 to 10 papillations, (3) 11 to 15 papillations, (4) about 16 to 25 papillations, and (5) >25 papillations. The data are shown elsewhere (J. Kurjan, Ph.D. thesis, University of Washington, Seattle, 1979). Most of the self-crosses show 0 to 2 papillations, but some cases showed up to 4 papillations. Thus, values 0 and 1 were taken to represent at most a very low frequency of recombination between the two sites.

For each mutation, the mutations with which it showed a recombination value of 0 or 1 were

TABLE 5. Qualitative meiotic recombination frequencies[a]

Cluster	Avg recombination value between clusters:									
	I	II	III	IV	V	VI	VII	VIII	IX	X
I	0.86	1.96	2.23	3.36	3.74	3.98	4.27	4.71	4.62	4.59
II	1.96	0.67	1.29	2.68	3.40	3.59	3.97	4.47	4.28	4.28
III	2.23	1.29	0.75	2.05	2.96	3.39	3.77	4.39	4.09	4.08
IV	3.36	2.68	2.05	0.71	2.00	3.29	3.45	4.25	4.09	4.23
V	3.74	3.40	2.96	2.00	0.80	3.20	3.60	3.95	4.07	4.17
VI	3.98	3.59	3.39	3.29	3.20	1.27	1.65	3.37	3.39	3.52
VII	4.27	3.97	3.77	3.45	3.60	1.65	0.52	2.71	3.07	3.20
VIII	4.71	4.47	4.39	4.25	3.95	3.37	2.71	1.00	2.60	3.32
IX	4.62	4.28	4.09	4.09	4.07	3.39	3.07	2.60	0.68	0.94
X	4.59	4.28	4.08	4.23	4.17	3.52	3.20	3.32	0.94	0.50

[a] The cluster-to-cluster recombination frequencies for the second meiotic fine-structure map are shown, with the order of the clusters being that determined for the final map. A definition of the recombination frequencies shown is in the text.

determined. The mutants could be divided into groups within which most crosses between any two mutants showed a background or close to background level of recombination with one another; the mutations could be grouped into 10 clusters. A number of mutations fit well into two clusters, and one mutation, M60, fits into three clusters. Other mutations showed very low recombination levels with a subset of the members of another cluster. These results indicate that the clusters overlap to some extent.

Ordering of the clusters into a map involved several steps. First, those clusters containing mutations from the first fine-structure map were placed according to their position on that map. Next, the remaining clusters were positioned on the new map, making use of the overlap between clusters described above. To adjust this map to give the most likely map order, it was necessary to determine distances between clusters based on the recombination values. Cluster-to-cluster recombination values were determined by averaging the recombination values (from 0 to 5) for all pairs of mutants between the two clusters, excluding the self-crosses in those cases in which a mutation was a member of both clusters. This gave a cluster-to-cluster distance between 0 to 5. Similarly, an intracluster recombination value for each cluster was determined by averaging the recombination values for all pairs of mutations within the cluster. These data are shown in Table 5 with the clusters arranged in the final order determined as was done for the first meiotic map. The final map is shown in Fig. 6, with the recombination values within clusters and between adjacent clusters shown. As one

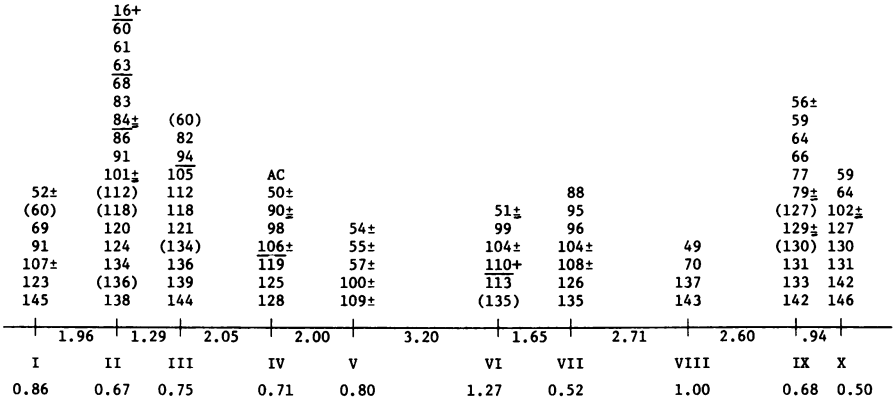

FIG. 6. Second meiotic fine-structure map. Distances between adjacent clusters are indicated between clusters, and the level of recombination between members of a cluster is indicated directly beneath the cluster. The background frequency for self-crosses is 0.29, as described in the text. Those mutants showing residual suppression are indicated by +, ±, or ±, as described in Table 1, footnote *b*. Mutants which show higher than normal recombination with two or more members of its cluster are underlined, and cases in which a mutant that maps to more than one cluster maps less well to a certain cluster are indicated by parentheses.

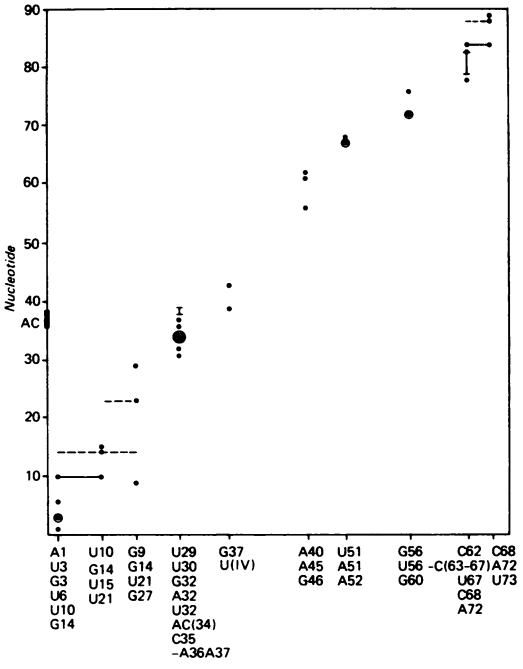

FIG. 7. Nucleotide position of the mutational changes versus meiotic fine-structure map 2, for those mutants for which the nucleotide alteration is known (10, 11). The results for 34 nucleotide alterations representing 40 of the 69 second-site mutants are shown. The position of the *SUP4* anticodon mutation is also indicated. The vertical bars represent mutation M77, which is a deletion of a single cytosine from a tract of five cytosines extending from nucleotide 79 to nucleotide 83, and mutation M119, which is a deletion of nucleotides 38 to 39. Horizontal bars connecting points represent cases in which a mutation maps equally well to two clusters. Horizontal dotted lines represent mutations which map well into the cluster indicated by the dot, but also map fairly well into an adjacent cluster. The circled dots represent different nucleotide changes at the same position.

cluster is compared with distal clusters, extreme map contraction is seen, due to the method of determining recombination values, since recombination value 5 has been scored as a single level of recombination although it actually represents a very large range of recombination frequencies.

The intracluster recombination values range from 0.50 to 1.27. If the recombination values (from 0 to 5) for the self-crosses are averaged in a manner similar to that used to determine both the intra- and intercluster values, the background value shown by the self-crosses is 0.29. The intracluster recombination values are all considerably higher than this background value, indicating that members of a cluster are not all identical. The different levels of residual suppression shown by members of a cluster, as illustrated in Fig. 6, again indicate that a cluster represents a group of nonidentical but presumably closely linked mutations. These differences in suppression properties along with the differences in mapping properties make this map very useful for distinguishing nonidentical mutants within clusters for various molecular studies of tRNA mutants.

Genetic map 2 versus physical structure. Figure 7 shows the correlation between the map positions of 41 of the 70 mutations mapped by the less quantitative method and their nucleotide positions within the gene. The 41 mutations include the *sup4*$^+$-*SUP4* alteration and 40 second-site mutations, which represent 34 nucleotide alterations, extending from the first to the last encoded nucleotide of the mature gene product. Again, the positions of the nucleotide changes show good correspondence with their map positions. All except one of the mutations show colinearity between their map location and the position of the nucleotide alteration. The one exception, mutant M105 (G9) (11), was mapped to cluster III, but its physical position is significantly closer to the 5′ end of the tRNA^{Tyr} than those of the other mutations in this cluster. This mutation shows a fairly low level of recombination with members of cluster I, but a higher level with some members of cluster II. Thus, the aberrant mapping of this mutation may be due to marker effects such that it gives unusually high levels of recombination with several members of cluster II. Those mutations which mapped to two adjacent clusters all lie between the other members of the two clusters. The one mutation which mapped to three clusters, M60, was shown to be a single base-pair substitution (11). Thus, this nucleotide alteration must result in a marker effect which leads to an unusually low level of recombination with surrounding mutations. Considering the quantitative nature of this mapping procedure and the problems with fine-structure mapping discussed above, the correspondence between map position and physical position is surprisingly good. These results indicate that the second mapping technique is accurate enough that once the nucleotide position of a number of mutants is known, the position within the tRNA^{Tyr} of other mutants on the map can be predicted with a fair degree of confidence to lie within a fairly small region of the gene.

DISCUSSION

In this paper we have described the isolation and characterization of second-site mutations at the *SUP4* locus which were obtained by selection for loss of suppression ability. The mutants show differing degrees of suppression loss, although all of the mutations of the *SUP4* gene

have lost most of the suppressor activity. However, the majority of the unlinked antisuppressors recovered in the mutant hunt were very leaky, showing a much higher level of residual suppression. Our selective technique allows the isolation of mutations which result in only a fairly slight loss of suppressor activity. However, we failed to recover mutations of this type at the *SUP4* gene, indicating that second-site mutations in the $tRNA^{Tyr}$ gene which only reduce tRNA function to a low degree are rare compared to mutations which have an extreme effect on tRNA function.

Meiotic fine-structure mapping of the mutants showed that the mutations map to many different positions within the gene. The first mapping technique placed 10 mutants plus the $sup4^+$ anticodon on a map by means of determining quantitative levels of recombination between pairs of mutations. This map showed many of the properties associated with fine-structure mapping in *S. cerevisiae*. One of these properties is map expansion, in which distant mutations result in a higher level of recombination than expected by the summing of the recombination frequencies for shorter intervals in between the two mutations. A possible explanation for map expansion is provided by a property observed in the study of gene conversion at the *arg4* locus (4). This study showed that the frequency of coconversion (versus single-site conversion) of two *arg4* heteroalleles was inversely proportional to the distance between the two alleles. Therefore, coconversion of close alleles will not be detected as a recombination event, whereas the single conversions for more distant alleles will result in recombinants.

Several of the mutations used in this mapping study showed marker effects, as described in Results. In addition, the recombination frequencies per nucleotide show considerable variation, with certain pairs of mutants showing frequencies either well below or well above the mean frequency of recombination per nucleotide. Marker effects such as these result in difficulties in the placement of mutations on the map. Despite all of these properties shown by the map, the correlation between the fine-structure map and the physical position of the mutations is quite good.

The second mapping technique utilized a more qualitative estimate of recombination frequency, allowing a large number of mutations to be mapped. The mutations were grouped into clusters within which the mutations showed very low recombination with one another. The recombination frequencies between pairs of clusters were determined by averaging the frequencies between all members of the two clusters, and the clusters were ordered with respect to one another based on these frequencies. At the time at which this map was completed, the nucleotide changes for only three mutations (M52, M50, and M77) were known; therefore this map provided a means by which to choose further mutants to clone and sequence which would be likely to lie throughout the tRNA gene. The position of the nucleotide changes for mutants chosen in this way show a surprisingly good correlation with this genetic map, with only one exception to colinearity of the map with physical position. We feel that the method used, which involved averaging of recombination frequencies for closely clustered mutations, may have resulted in the averaging of marker effects, therefore eliminating some of the problems that these marker effects cause in the construction of a fine-structure map.

Thus, although it is clear that the gene studied in this paper shows some of the problems associated with fine-structure mapping (marker effects and map expansion), the results presented here indicate that the map shows a high degree of correspondence with nucleotide position. The maps have already been very useful tools for choosing mutants for further study, allowing a choice of mutations in parts of the gene of particular interest. Various experiments have begun to categorize the mutants with respect to their defect, which could lie at the level of transcription, processing and modification of the primary transcript, or various aspects of tRNA function, such as ribosome binding or aminoacylation (8, 10).

ACKNOWLEDGMENTS

We thank Rodney Rothstein for many helpful discussions during the course of this work. We also thank Rodney Rothstein and Anita Hopper for comments on the manuscript.

This research was supported by Public Health Service research grant GM-11895 from the National Institutes of Health. J.K. was a National Institutes of Health predoctoral trainee in Genetics.

LITERATURE CITED

1. **Celis, J. E.** 1979. Collection of mutant tRNA sequences. Nucleic Acids Res. 1:r21–r27.
2. **Cooper, T. G., C. Lam, and V. Turoscy.** 1980. Structural analysis of the *dur* loci in *Saccharomyces cerevisiae*: two domains of a single multifunctional gene. Genetics **94**:555–580.

2a. **DiCaprio, L., and P. J. Hastings.** 1976. Gene conversion and intragenic recombination at the SUP6 locus and the surrounding region in *Saccharomyces cerevisiae*. Genetics **84**:697–721.

3. **Esposito, M. S.** 1968. X-ray and meiotic fine structure mapping of the adenine-8 locus in *Saccharomyces cerevisiae*. Genetics **58**:507–527.
4. **Fogel, S., and R. K. Mortimer.** 1969. Informational transfer in meiotic gene conversion. Proc. Natl. Acad. Sci. U.S.A. **62**:96–103.
5. **Grenson, M., M. Mousset, J. M. Wiame, and J. Bechet.** 1966. Multiplicity of the amino acid permeases in *Saccharomyces cerevisiae*. I. Evidence for a specific arginine-

transporting system. Biochim. Biophys. Acta 127:325–338.
6. **Hofer, F., H. Hollenstein, F. Janner, M. Minet, P. Thuriaux, and U. Leupold.** 1979. The genetic fine structure map of nonsense suppressor in *Schizosaccharomyces pombe*. I. *sup*3 and *sup*9. Curr. Genet. 1:45–61.
7. **Holliday, R.** 1964. A mechanism for gene conversion in fungi. Genet. Res. 5:282–304.
8. **Hopper, A. K., and J. Kurjan.** 1981. tRNA synthesis: analysis of *in vivo* precursor tRNAs from wild-type and mutant yeast strains. Nucleic Acids Res. 9:1019–1029.
9. **Jones, E. W.** 1972. Fine structure analysis of the *ade*3 locus in *Saccharomyces cerevisiae*. Genetics 70:233–250.
10. **Koski, R. A., S. G. Clarkson, J. Kurjan, B. D. Hall, and M. Smith.** 1980. Mutations at the yeast *SUP*4 $tRNA^{Tyr}$ locus: transcription of the mutant genes *in vitro*. Cell 22:415–425.
11. **Kurjan, J., B. D. Hall, S. Gillam, and M. Smith.** 1980. Mutations at the yeast *SUP*4 $tRNA^{Tyr}$ locus: DNA sequence changes in mutants lacking suppressor activity. Cell 20:701–709.
12. **Messenguy, F. R., and G. R. Fink.** 1973. Temperature-sensitive nonsense suppressors in yeast. Genetics 75:459–464.
13. **Moore, C. W., and F. Sherman.** 1975. Role of DNA sequences in genetic recombination in the *iso*-1-cytochrome c gene of yeast. I. Discrepancies between physical distances and genetic distances determined by five mapping techniques. Genetics 79:397–418.
14. **Moore, C. W., and F. Sherman.** 1977. Role of DNA sequences in genetic recombination in the *iso*-1-cytochrome c gene of yeast. II. Comparison of mutants altered at the same and nearby base pairs. Genetics 85:1–22.
15. **Mortimer, R. K., and D. C. Hawthorne.** 1969. Yeast genetics, p. 386–460. *In*, A. H. Rose and J. S. Harrison (ed.), The yeasts, vol. 1. Academic Press, Inc., New York.
16. **Olson, M. V., G. S. Page, A. Sentenac, K. Loughney, J. Kurjan, J. Benditt, and B. D. Hall.** 1980. Yeast suppressor tRNA genes, p. 267–279. *In* D. Söll, J. Abelson, and P. R. Schimmel (ed.), Transfer RNA: biological aspects, part B. Cold Spring Harbor Laboratory, Cold Spring Harbor, N.Y.
17. **Rothstein, R. J.** 1977. A genetic fine structure analysis of the suppressor 3 locus in *Saccharomyces*. Genetics 85:55–64.
18. **Rothstein, R. J.** 1979. Deletions of a tyrosine tRNA gene in *Saccharomyces cerevisiae*. Cell 17:185–190.
19. **Rothstein, R. J., R. E. Esposito, and M. S. Esposito.** 1977. The effect of ochre suppression on meiosis and ascospore formation in *Saccharomyces*. Genetics 85:33–54.
19a. **Sprinzl, M., F. Grueter, A. Spelzhaus, and D. H. Gauss.** 1980. Compilation of tRNA sequences. Nucleic Acids Res. 8:r1–r22.
20. **Yanofsky, C., B. C. Carlton, J. R. Guest, D. R. Helinski, and U. Henning.** 1964. On the colinearity of gene structure and protein structure. Proc. Natl. Acad. Sci. U.S.A. 51:266–272.